Wet Gas Metering with the V-Cone and Neural Nets

Haluk Toral and Shiqian Cai
Petroleum Software Ltd.
Robert Peters
McCrometer

Abstract

The paper presents analysis of extensive measurements taken at NEL, K-Lab and CEESI wet gas test loops. Differential and absolute pressure signals were sampled at high frequency across V-Cone meters. Turbulence characteristics of the flow captured in the sampled signals were characterized by pattern recognition techniques and related to the fractions and flow rates of individual phases. The sensitivity of over-reading to first and higher order features of the high frequency signals were investigated qualitatively. The sensitivities were quantified by means of the saliency test based on back propagating neural nets. A self contained wet gas meter based on neural net characterization of first and higher order features of the pressure, differential pressure and capacitance signals was proposed. Alternatively, a wet gas meter based on a neural net model of just pressure sensor inputs (based on currently available data) and liquid Froude number was shown to offer an accuracy of under 5% if the Froude number could be estimated with 25% accuracy.

Introduction

Wet gas measurements were conducted under a wide range of conditions with a V-cone meter in the test loops at NEL, K-Lab and CEESI. Measurements, comprising high frequency signals from pressure and differential pressure sensors, were analysed by characterisation of the turbulence properties of the flow by means of a pattern recognition / neural net methodology described in previous publications [1,2]

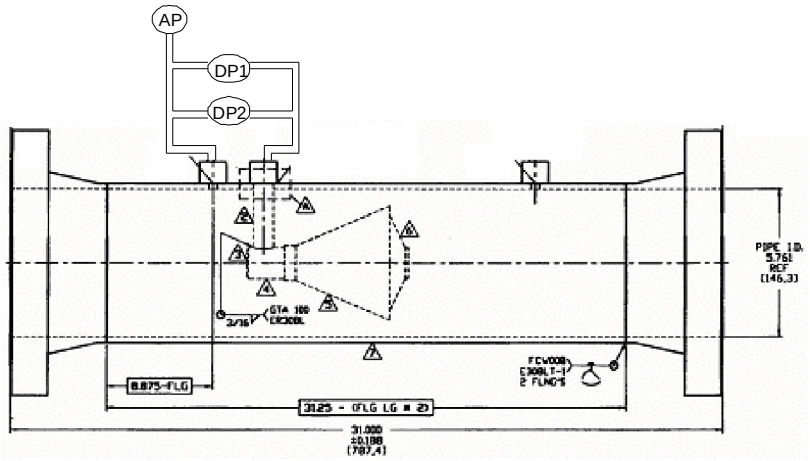

DP1: Standard DP
DP2: ESMER Fast DP
AP: ESMER Fast AP

Figure 1. Schematic Diagram of V-Cone

The V-cone was connected to high frequency absolute and differential pressure gauges and a portable PC as the data acquisition system. The signals were sampled and analysed by extracting characteristic features from fluctuating differential and pressure signals sampled at high frequencies. Examples of such features can be given as standard deviation in the amplitude domain and linear prediction coefficients in the frequency domain. The efficiency of the features for discriminating between different flow conditions is assessed by means of the Saliency test. The features were then related to the superficial velocities of individual phases by means of a back-propagating neural net. A data flow diagram of the concept is shown in figure below.

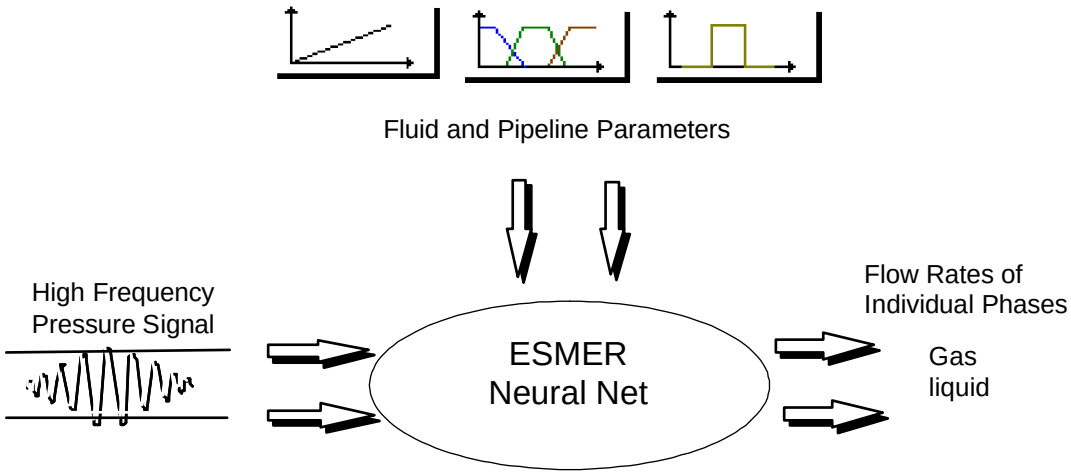

Figure 2. Schematic diagram of the ESMER concept

Test matrices covered a range of flow conditions up to 15% liquid volume fraction, operating pressure up to 90 bar; gas actual volumetric flow of 1000 m3/hr. Kerosene, condensate, field gas and nitrogen was used in different labs in 4" and 6" lines. The chart below gives a graphic summary of the flow conditions.

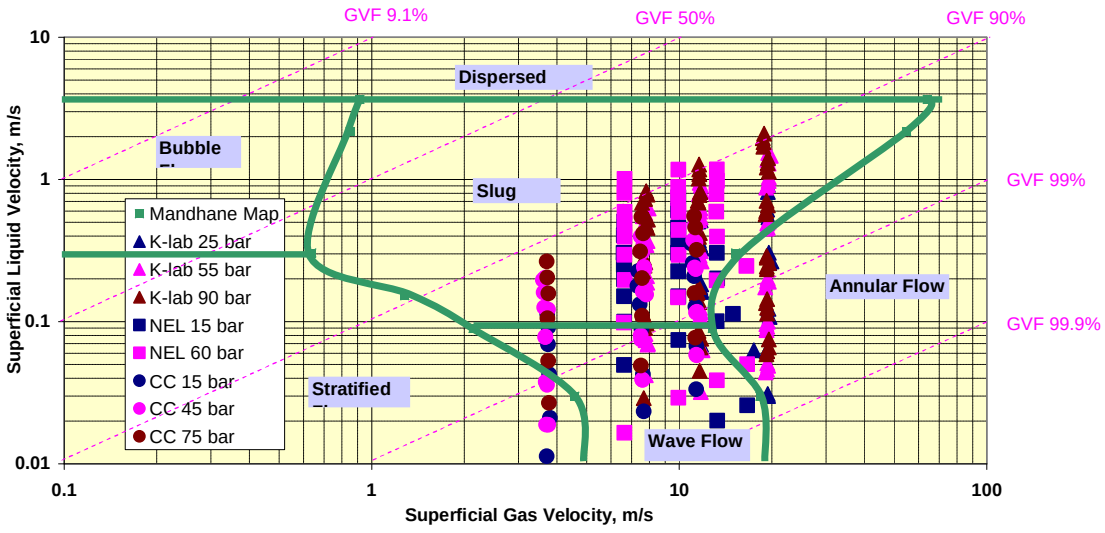

Figure 3. Operating envelope of NEL, K-lab and CEESI test data

Qualitative Analysis

We have started the analysis with the conventional *overreading* graph. Briefly, this graph shows the effect of the liquid fraction on the differential pressure measured across the V-Cone. The liquid fraction is quantified by means of the Lockhart Martinelli number as the ratio of liquid momentum to gas momentum expressed as:

$$X = \frac{m_l}{m_g}\sqrt{\frac{\rho_g}{\rho_l}}$$

and the differential pressure across the V-cone is non-dimensionalised with the theoretical dry gas differential pressure expressed as:

Over-reading = $\sqrt{\Delta p / \Delta p_g}$

where :

Δp_g = theoretical differential pressure across the V-cone calculated from the standard V-cone equation based on (reference) superficial gas velocity [3]

Overreading is partly due to the presence of the liquid phase (greater mixture density than that assumed by the application of the dry gas equation) and partly due to greater frictional losses in the throat of the V-Cone as a result of interfacial interactions between the segregated phases as explained long ago by Lockhart Martinelli [4]

"The pressure drop in the two phase flow is greater than that for the flow of either single phase alone for various reasons, among which are the irreversible work done by the gas on the liquid and the fact that the presence of the second fluid reduces the cross sectional area of flow for the first fluid. Thus during two-phase flow the hydraulic diameters Dl and Dg are always less than the pipe diameter Dp as noted in the Fanning equations…, this reduction of hydraulic diameter will increase the pressure drop greatly."

The overreading graph shows a wide scatter when all data points are included for measurements taken in all laboratories. For example, figure 4a shows the overreading graph for NEL and figure 4b shows the overreading graph for K-Labs.

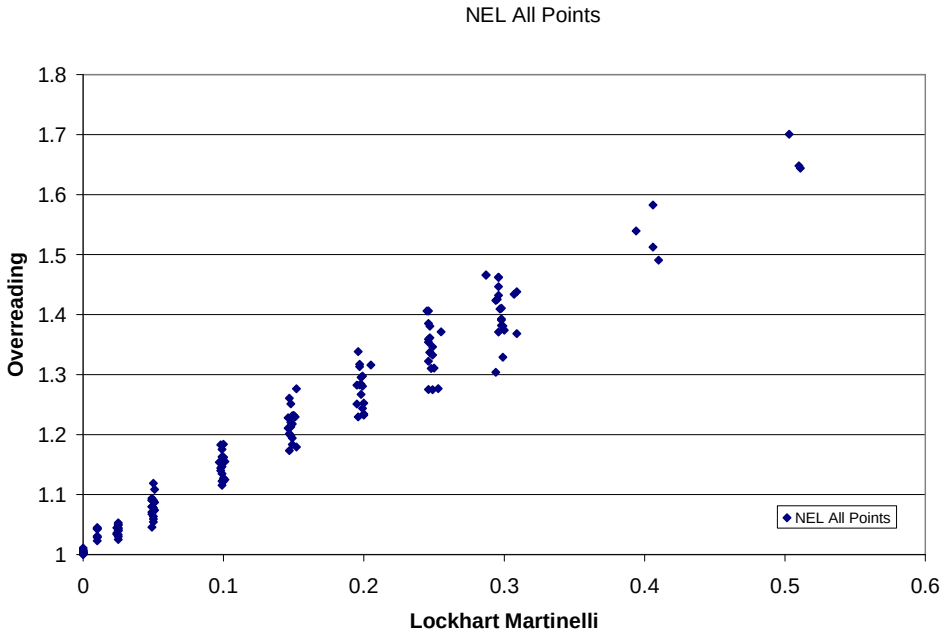

Figure 4 a.Overreading graph for data collected at NEL

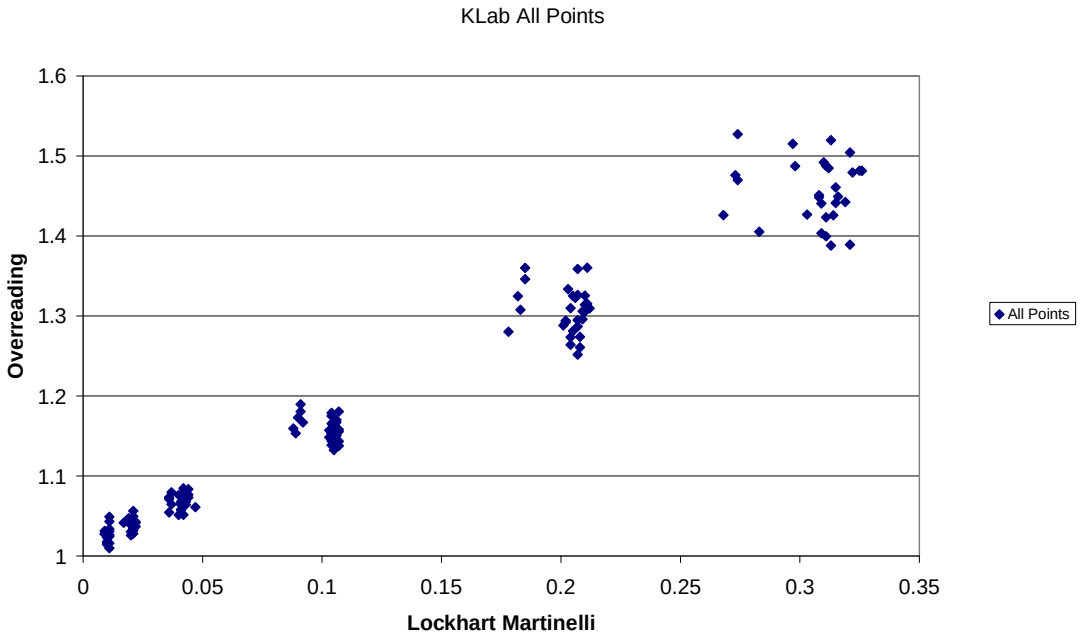

Figure 4 b.Overreading graph for data collected at K-Labs

We have considered a number of possible reasons for the scatter on these graphs including:

- variation in the physical properties
- variation in the density of fluids
- flow regime effects
- experimental error
-

As the physical properties of the fluids are constant at each laboratory, variation in the physical properties can be ruled out as an explanation of the scatter.

Density variations were considered next. As the tests were carried out with the same liquid in each series of tests, we only had to consider the effect of variation in the density of the gas. We have used pressure as a surrogate for examining this effect. Figure 5a for NEL and figure 5b for K-labs shows that density / pressure has a definite effect on the scatter.

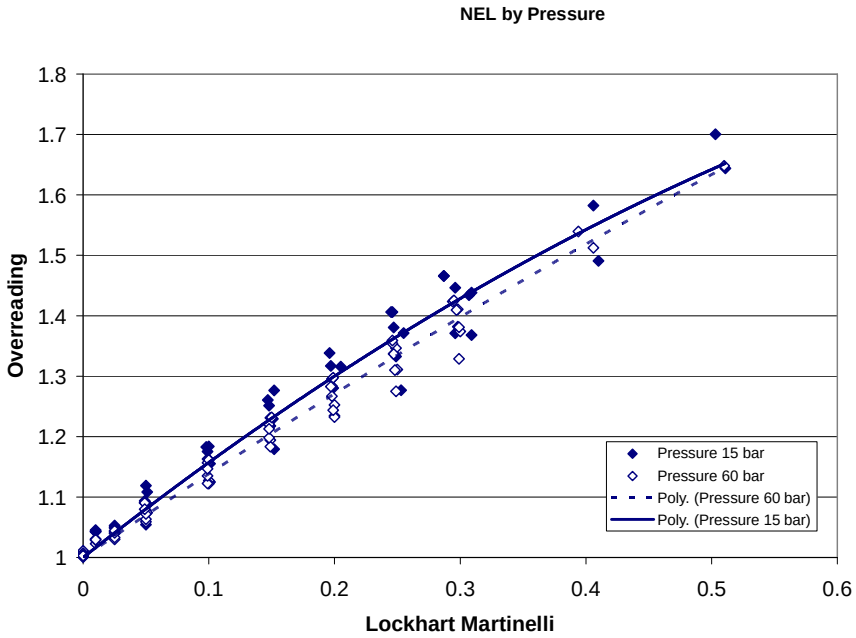

Figure 5 a.Overreading graph for data collected at NEL at different pressures

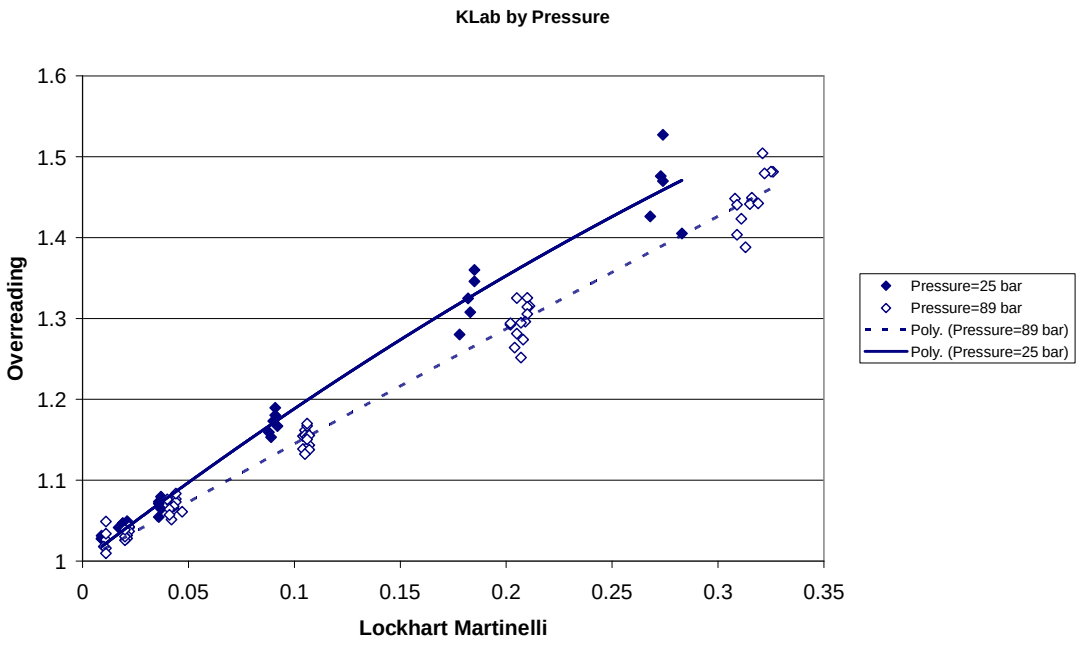

Figure 5 b.Overreading graph for data collected at K-Labs at different pressures

It is seen that overreading increases with decreasing pressure (ie gas density) at the same Lockhart Martinelli number. This can be explained as greater turbulence, and

hence greater interfacial frictional losses arising from the commingled flow of phases of larger density difference.

We have next examined the flow regime effect in further depth. The flow regime effect is of course already taken into account by the Lockhart Martinelli number as a first order effect. The ratio of liquid to gas momentum will exert a decisive effect on the flow regime. The density effect mentioned above can also be considered as a second order flow regime effect.

However, there is another factor at work in establishing the finer characteristics of the flow regime at a given Lockhart Martinelli number and pressure (gas density). This is the ratio of the axial momentum (of the liquid or the gas phase) to gravitational force arising from the difference in density of gas and liquid phases. The Froude number provides the mathematical expression to this ratio. Figures 6a for NEL and figure 6b for K-Labs shows the scatter caused by the variation in Froude number within given Lockhart Martinelli bands. The overreading increases with increasing Froude number because of greater turbulence effects giving rise to larger frictional pressure loss. As expected the Froude number effect was observed to diminish with increasing pressure.

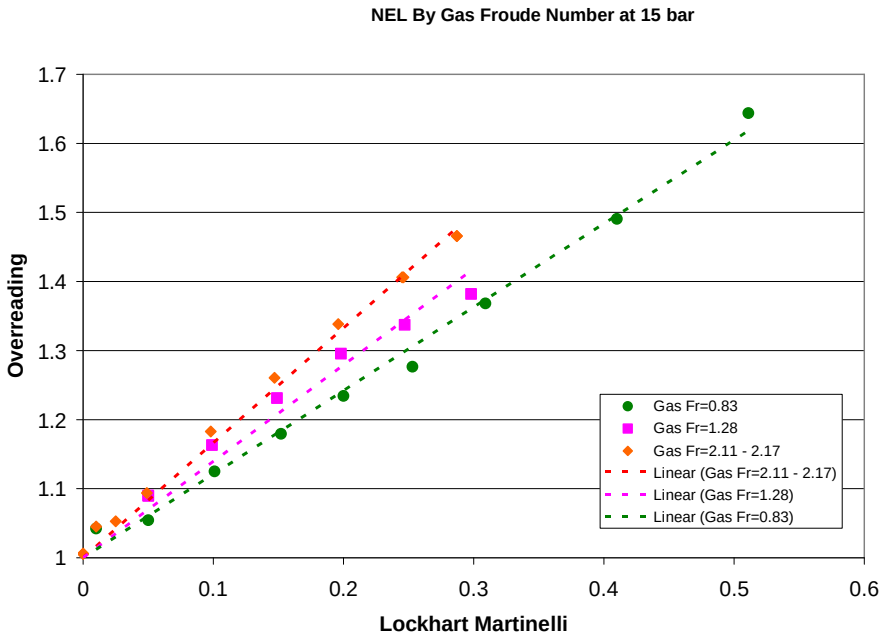

Figure 6 a.Overreading graph for data collected at NEL at different Froude number

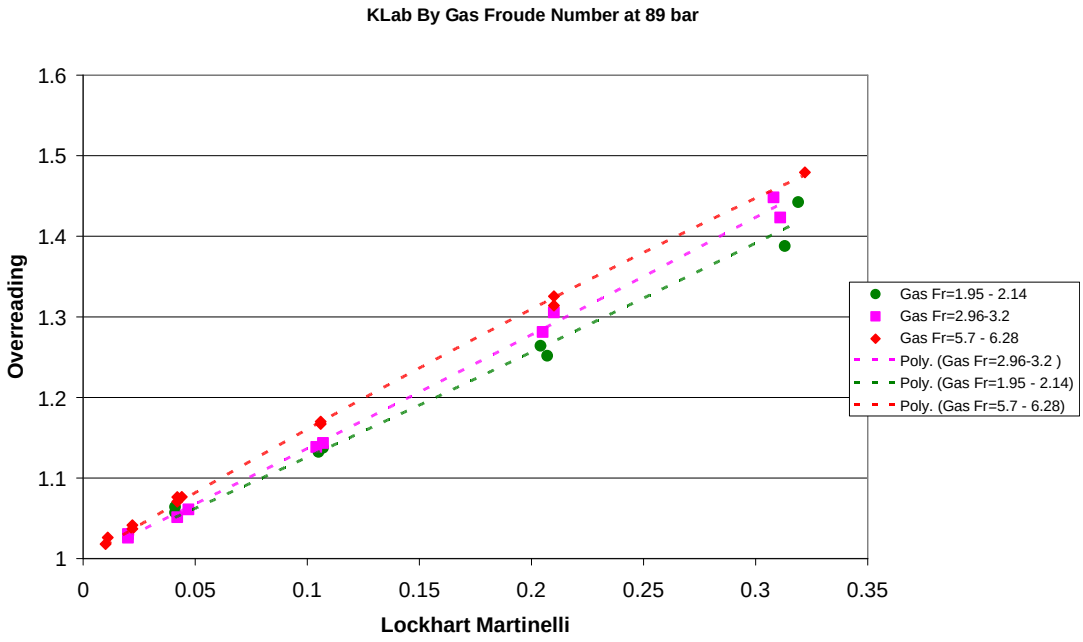

Figure 6 b.Overreading graph for data collected at K-Labs at different Froude number

The importance of the Froude number was highlighted when comparing the results from two labs at the same Froude number. For example, figure 7a, shows two sets of data drawn from NEL at different Froude numbers. As normal, the overreading increases with Froude number. However, the graph of overreading drawn from K-Labs measurements coincide with that from NEL at the same Froude number. This finding confirms the importance of Froude number as a first order effect and also indicates that experimental error is of lesser importance as an explanation of scatter.

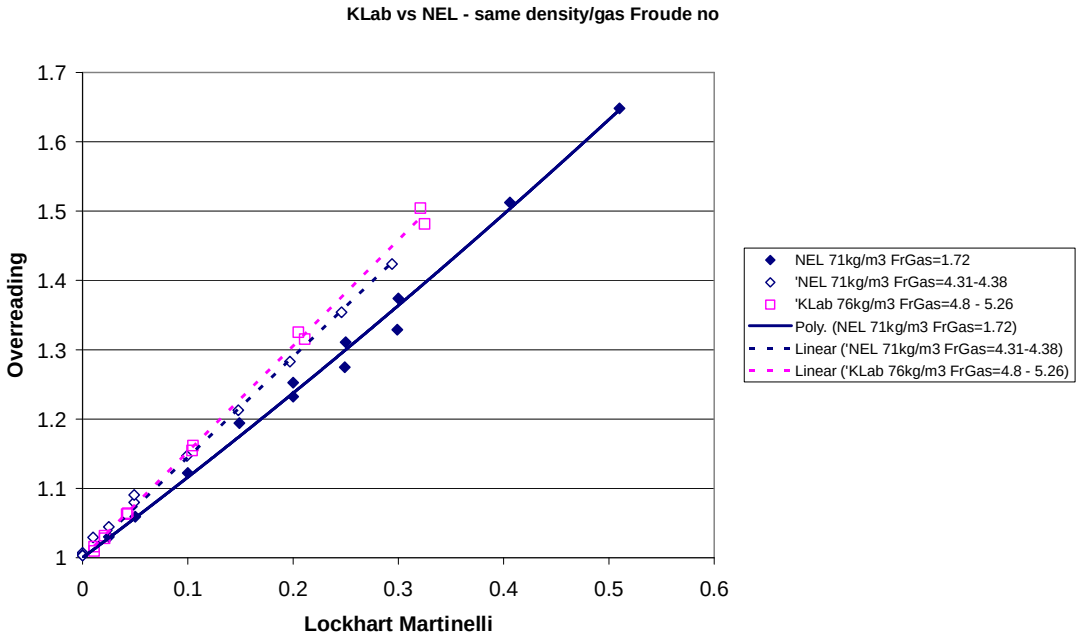

Figure 7 a.Overreading graph for data collected at K-Labs and NEL at same Froude number

The same observation is repeated in figure 7b which shows two sets of data drawn from CEESI at different Froude number against one data set drawn from K-labs at the same Froude number as one of the CEESI data sets. Once again the graphs of overreading at same Froude number coincide irrespective of where the data is coming from.

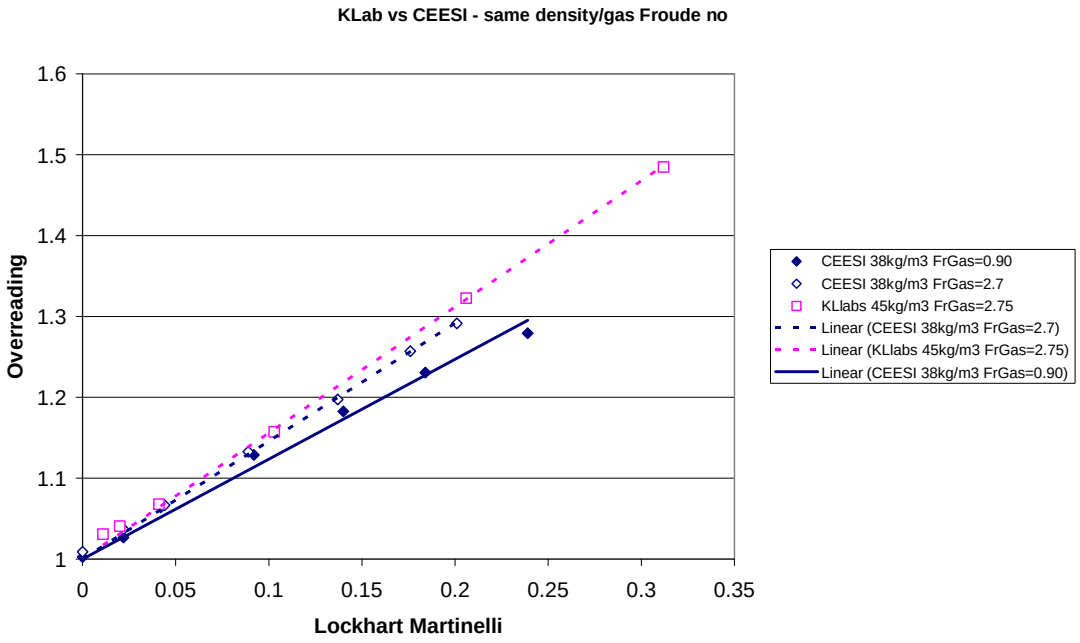

Figure 7 b.Overreading graph for data collected at K-Labs and CEESI at same Froude number

Quantitative Analysis by Neural Nets

The Froude number effect was noted previously; eg see [3], and no claim is made in this paper for originality for noting the effect. However, we believe that the method outlined next for quantifying this effect in relation with others is original to this paper.

After the qualitative analysis described above, we proceeded to carry out a quantitative analysis of the sensitivity of over-reading to various parameters. We have used a back propagating neural net and tried different features, targets and training data. Two configurations of the neural net are reported here. For both configurations, the neural net had eight input nodes and 16 hidden nodes, but different sets of inputs (features) and outputs (targets) were tried as follows

Neural Net 1 Features: The following features were used as input variables (codes are used for reference to figure 9) :

F70:	Liquid Froude Number
X	Lockhart Martinelli parameter
F48:	Gas Froude Number
F53:	$\sqrt{\frac{\Delta p}{\rho_g}}$
F43:	$\sqrt{\frac{\Delta p}{\rho_m}}$
F37:	$\sqrt{\Delta p}$
F69:	$\sqrt{\frac{\Delta p}{\rho_l}}$
Pressure	P

Neural Net 1 Targets: Over-reading was used as the training target.

Neural Net 1 Data: NEL data was used for training and testing. The self test result of the neural net is shown in figure 8. The deviation between actual and prediction was 0.0013 rms

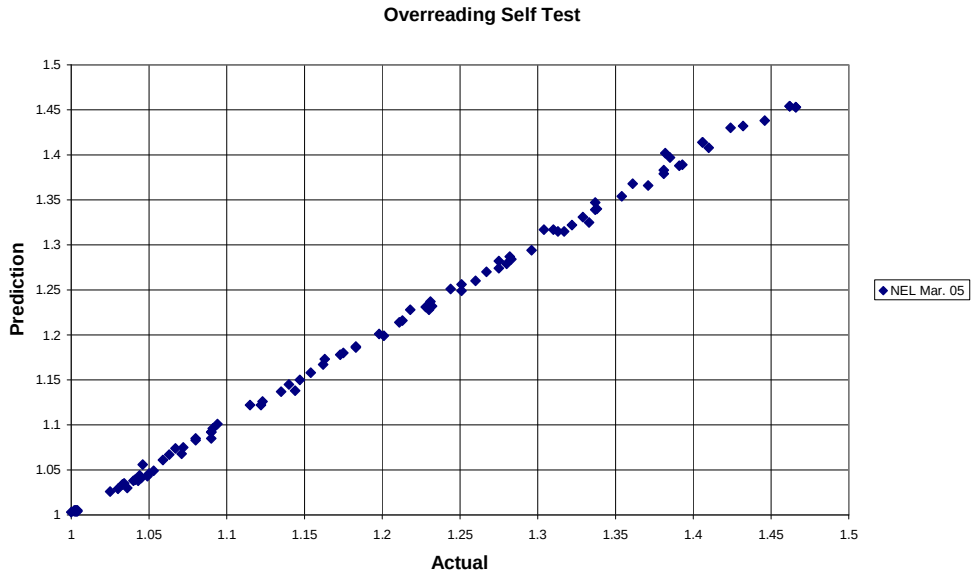

Figure 8 Neural net self test overreading predicted vs overreading actual

We then carried out the saliency test to obtain a quantitative measure of the sensitivity of over-reading to the input parameters [4]. The result of the saliency test is shown on figure 9.

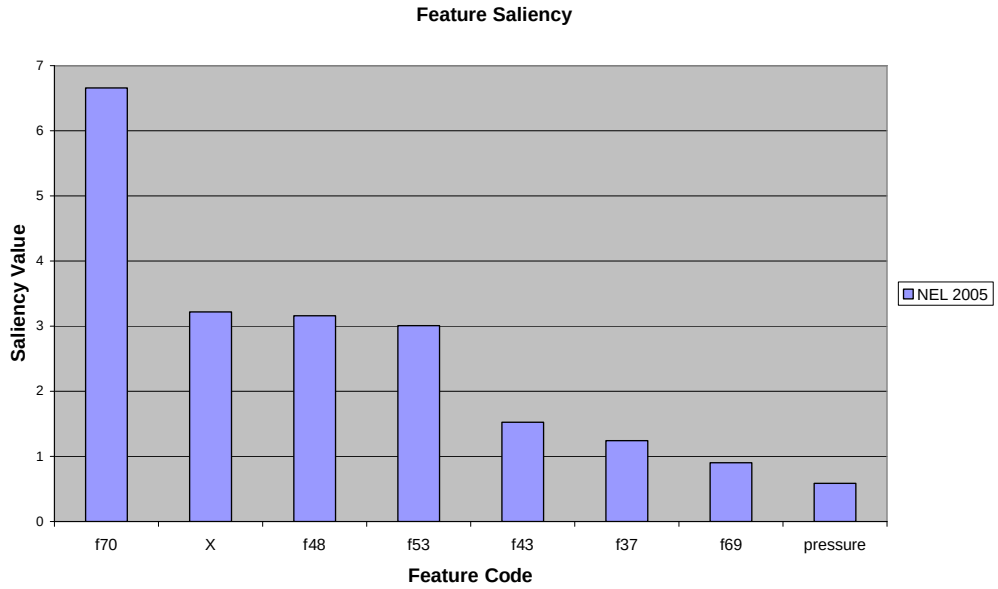

Figure 9 Saliency test neural net 1 – sensitivity of various parameters on overrreading

Neural Net 2 Features:

F65 = $\sqrt{\frac{\Delta p}{P}}$

F53: $\sqrt{\frac{\Delta p}{\rho_g}}$

F37: $\sqrt{\Delta p}$

F70: Liquid Froude Number

F69: $\sqrt{\frac{\Delta p}{\rho_l}}$

Pressure
Density Gas
Density Liquid

Neural Net 2 Targets: Neural net 2 was trained against liquid and gas superficial velocities (two targets).

Neural Net 2 Data: Self test and cross test results for this neural net with two sets of NEL data obtained at different times (May 03 and March 05) is shown below:

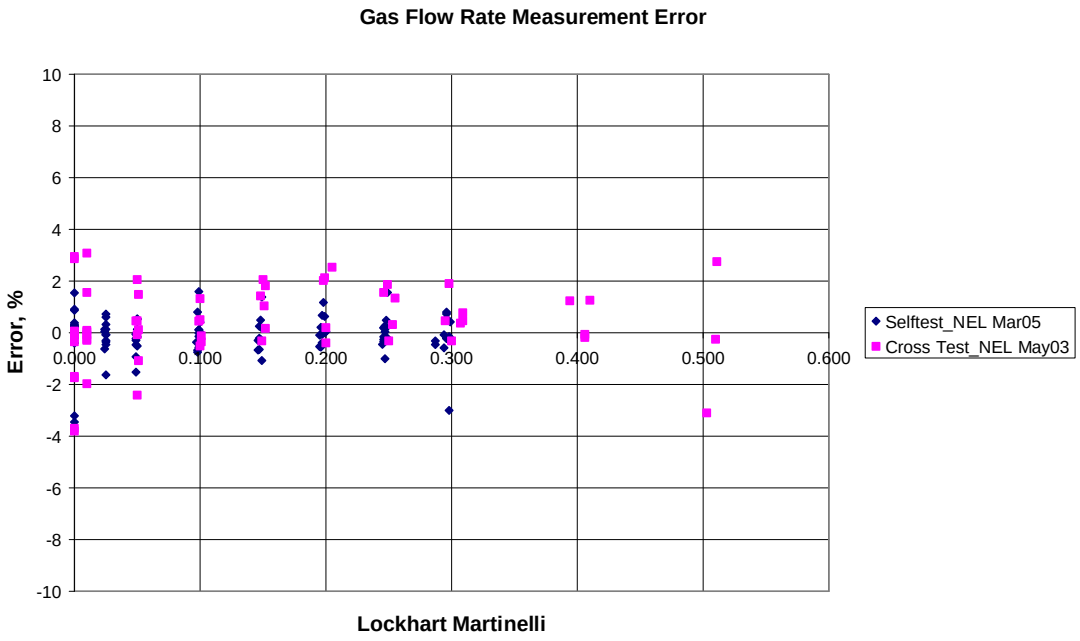

Figure 10 Error in prediction of the gas flow rate with neural net 2 – cross test

The neural net was trained with data gathered in March 05 and back tested against data gathered in May 03. The gas superficial velocity was predicted with an accuracy of rms 1.51 and liquid superficial velocity was predicted with an accuracy of rms 13.74.

The sensitivity of the predictions to input features are shown in figure 11.

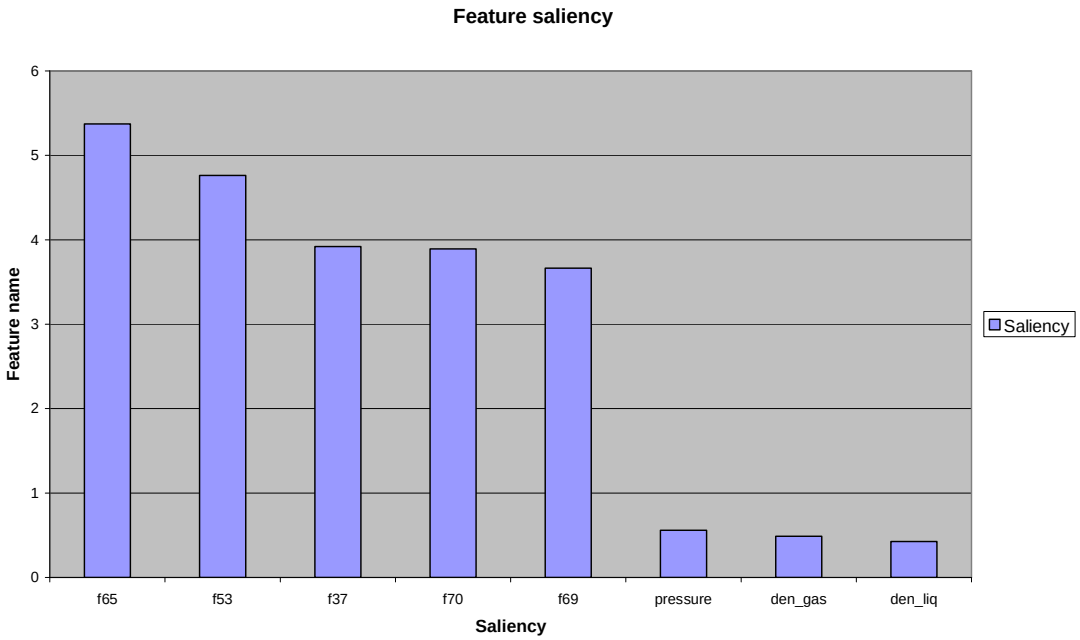

Figure 11 Saliency test neural net 1 – sensitivity of various parameters on liquid and gas superficial velocity prediction

Wet Gas Flow Meter

The brief of an in-line wet gas flow meter is to measure liquid and gas flow rates simultaneously. This requires two measurements (equations) responding in two different ways to the flow rate of liquid and gas flow rate (to solve for two unknowns). One of these measurements (equations) is the mean differential pressure across the V-Cone (Bernoulli equation - momentum balance with appropriate compensation for additional frictional pressure loss arising from interfacial interaction). Another equation can be obtained either from pressure recovery downstream of the V-Cone or from another V-Cone with a different beta ratio. These ideas have been tried before with varying degrees of success.

Another possibility is to extract some features from the differential pressure sampled at a high frequency which respond to the liquid fraction or to the change in liquid and gas flow rates differently. That is, to derive two simultaneous equations from the same measurement. This was tried in the present study. To see how features vary differently to liquid and gas rates we have plotted contour maps of features extracted from the differential pressure signal.

When contours of features are plotted on superficial velocity coordinates one must obtain "intersection" between different feature surfaces (for a solution to the equations) For example, it is not enough to have contours which are laid out diagonally (eg mean DP, standard deviation are typical examples of diagonal contours which do not intersect). Depending on the angle of the diagonal, intersection is still possible (eg variation of mean DP with liquid and gas flow rates is concave but variation of higher order amplitude domain features such as standard deviation, coefficient of kurtosis are convex); but the sharper the angle the better chance for intersection (ie angle =0 -> horizontal contours; angle = 90 vertical contours; angle=45 diagonals).

Figure 12 shows some of the amplitude domain features extracted from the differential pressure signal. These features were extracted from tests conducted at NEL in May 03.

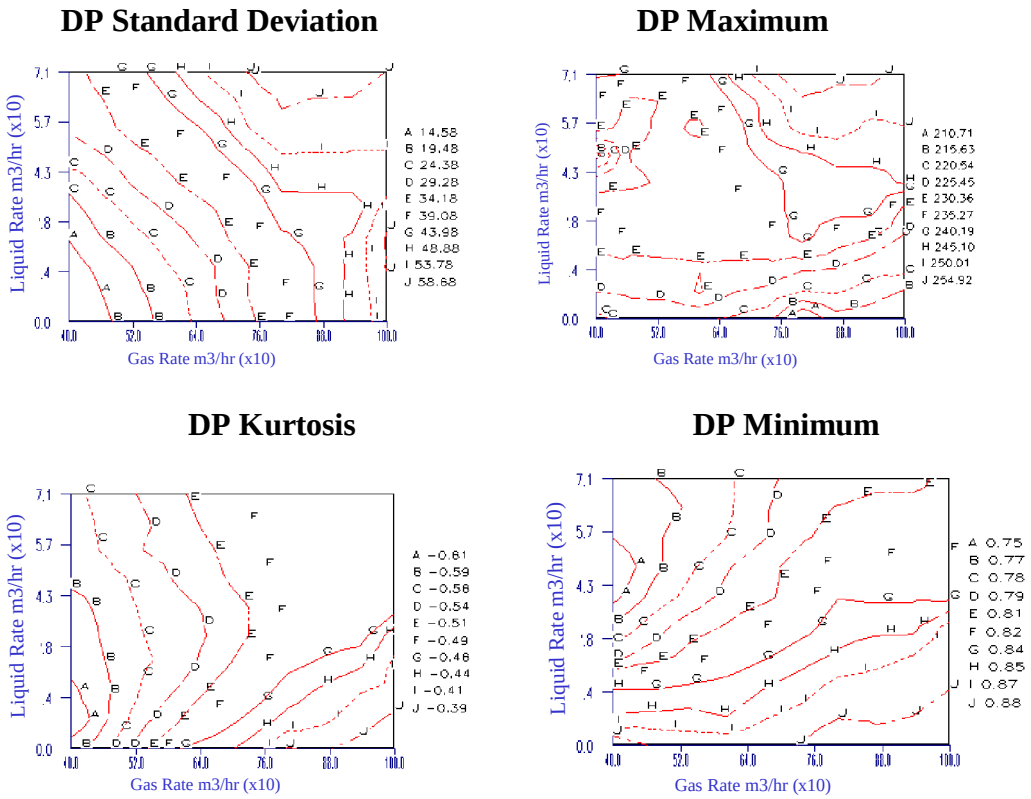

Figure 12 Differential pressure second order features amplitude domain as contour maps on liquid / gas flow rate coordinates.

We have found that while multiple features from the differential pressure provide the intersection points required for identifying liquid and gas rates simultaneously in a given pipeline (or flow loop), for generalization of this method, a stronger (reproducible) imprint of the flow characteristics is necessary. For this it is necessary to add features extracted from another sensor which responds directly to the presence of the liquid phase. For example features extracted from a capacitance sensor in figure 13 show that the capacitance feature surface will intersect with the differential pressure features (eg mean DP rising towards North East, whereas mean capacitance rising towards North West, etc – one can see similar reverse trends in a number of other stochastic features extracted from the respective signals). The measurements shown in figure 13 were made in NEL multiphase flow loop in 1999 – NEL Multiflow JIP [5]

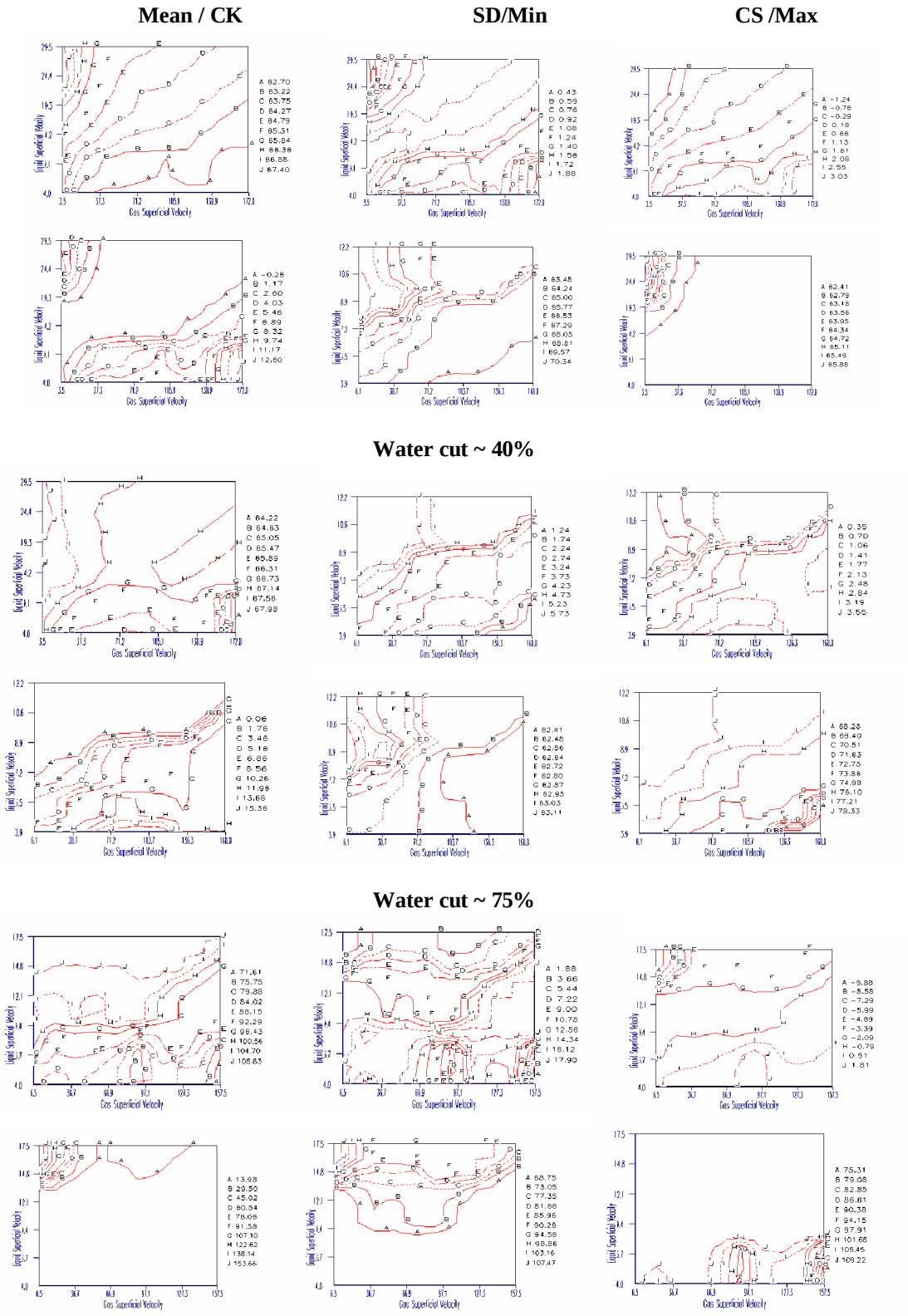

Figure 13 Capacitance sensor second order features amplitude domain as contour maps on liquid / gas flow rate coordinates.

Thus a combination of DP and capacitance sensors will result in a metering system with a greatly enhanced capability for the identification of liquid and gas rates. It can be seen from the trends in contour maps that input-output relations are non-linear and multi-

parameter (eg mean capacitance is not just affected by water composition but also by flow regimes which are in turn affected by superficial velocities and density difference, etc). We believe that only a neural net is capable of finding the relationship between the complex set of causes and effects in multiphase flow.

Finally, we believe that there are still many advantages to the conventional overreading correction approach coupled with a neural net method for correlation of the experimental database. This method of course requires an independent measurement of the Froude number (see Neural Net 2 above). However, an estimate of the liquid Froude number can still result in a relatively good measurement (it is not in the brief of this paper to suggest how this estimate can be made, but a number of options are available including tracers, equation of state, production separator, etc). For example, we have tested the neural net (cross test with erroneous Froude numbers and obtained the result shown in figure 14. It is seen that the rms error in gas prediction is rms 1.51 when the neural net is tested with the correct Froude number. The error goes up to rms 9.13 when Froude number is out by 50% ie when (FrEstimated – FrActual)/FrActual x 100 =50% (figure 14a).

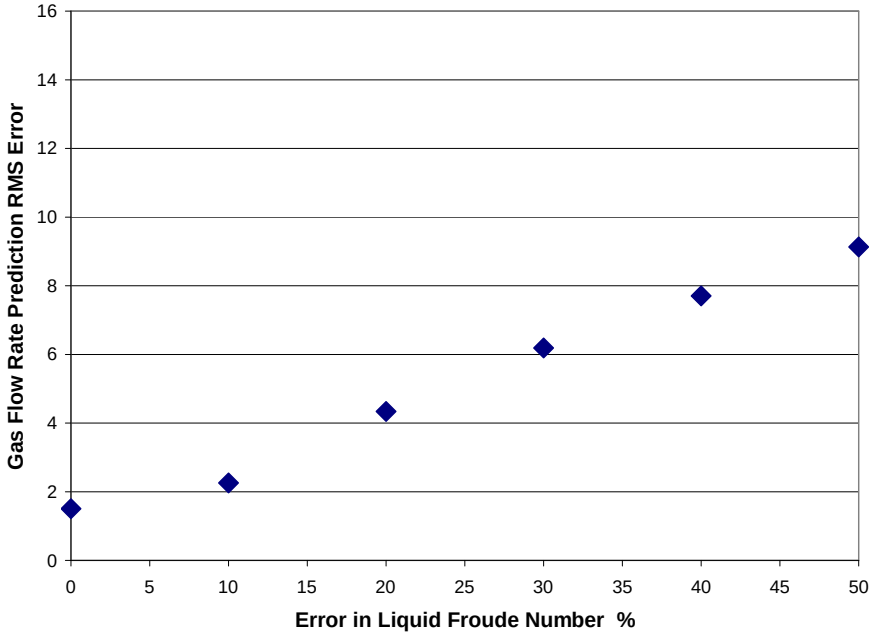

Figure 14a Error in gas rate prediction versus error in liquid Froude number (Neural Net 2)

An interesting byproduct of this investigation was the finding shown in figure 14b that the prediction made by the neural net for the liquid rate is actually better than the input value for Froude number error greater than 20% (Note that this neural net has two targets and the liquid rate is used both as an input feature – via liquid Froude number- and as an output target.)

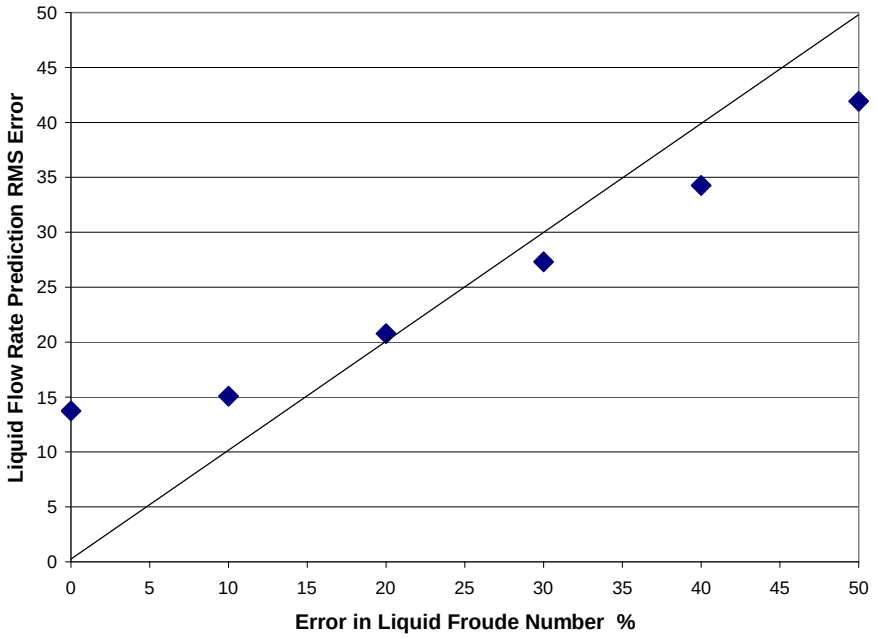

Figure 14b Error in liquid rate prediction versus error in liquid Froude number (Neural Net 2)

Conclusions

1. Back propagating neural nets present a powerful tool for investigating cause and effect relations in wet gas. The effect of Froude number on overreading ratio was quantified by analyzing measurements conducted with V-cones under a wide range of conditions at different laboratories.

2. Back propagating neural nets can also be used as kernel software in a self contained wet gas flow metering system. If the wet gas meter comprises just a V-Cone coupled with a differential pressure sensor and pressure sensor, the liquid Froude number must be input explicitly. In this configuration, the neural net can be self-contained (ie can predict both liquid and gas rates simultaneously) in a given pipeline after suitable training.

3. A general wet gas metering system (ie simultaneous self-contained measurement of liquid and gas rates from a factory calibration) is possible with a combination of differential pressure and capacitance sensors and a neural net for correlating the complex causes and effects between hydrodynamics and phase distributions.

4. A general wet gas metering system is also possible with a neural net trained with features extracted from just the pressure sensors and an external input for liquid Froude number. The error in the gas rate prediction made by the neural net will be under 5% for an error in the Froude number of 25%.

Notation

ρ_l = liquid density

ρ_g = gas density

v_g = superficial gas velocity

Δp_g = theoretical differential pressure across the V-cone calculated from the standard V-cone equation based on (reference) superficial gas velocity

Δp = actual differential pressure across the V-cone (measured)

Frl=Liquid Froude Number = V_l/Sqrt(9.81*Diameter)*Sqrt(ρ_l /(ρ_l - ρ_g)

FrG = Gas Froude Number =Vg/Sqrt(9.81*Diameter)*Sqrt(ρ_g /(ρ_l - ρ_g)

References

[1] Haluk Toral, Shiqian Cai, Richard Steven, Robert Peters, Characterization of the turbulence properties of wet gas flow in a V-Cone meter with neural nets 22nd North Sea Flow Measurement Workshop October 2004 St Andrews

[2] Shiqian Cai, Haluk Toral, Dasline Sinta, Meramat Tajak Experience in field tuning and operation of a multiphase meter based on neural net characterization of flow conditions, (Sarawak Shell Bhd Malaysia) FLOMEKO 2004 Beijing 14-17 Sept. 2004

[3] David Steward, David Hodges, Richard Steven, Robert Peters Wet gas Metering with V-Cone Meters 20th North Sea Flow Measurement Workshop October 2002 St Andrews

[4] Lockhart R.W. , Martinelli R.C."Proposed Correlation of Data for Isothermal Two-Phase Two Component Flow in Pipes" Chemical Engineering Progress Vol 45 No 1

[5] Priddy K. L., Rogers S. K., Ruck D. W., Tarr G. L., and Kabrisky M. (1993) "Bayesian selection of important features for feedforward neural networks," Neurocomputing, vol. 5, no. 2--3, pp. 91--103. http://citeseer.ist.psu.edu/priddy93bayesian.html

[6] A Hall NEL Multiflow JIP Evaluation of ESMER T3 Multiphase Flow Meter 30 March 2000 National Engineering Laboratory Report 069/2000